Crystal structure of apo-calmodulin bound to the first two IQ motifs of myosin V reveals essential recognition features

Anne Houdusse, Jean-François Gaucher, Elena Krementsova, Suet Mui, Kathleen M. Trybus, and Carolyn Cohen

PNAS 2006;103;19326-19331; originally published online Dec 6, 2006;
doi:10.1073/pnas.0609436103

Crystal structure of apo-calmodulin bound to the first two IQ motifs of myosin V reveals essential recognition features

Anne Houdusse*, Jean-François Gaucher†, Elena Krementsova‡, Suet Mui§¶, Kathleen M. Trybus‡‖, and Carolyn Cohen§‖

*Motilité Structurale, Institut Curie, Centre National de la Recherche Scientifique, Unite Mixté de Recherche 144, 26 rue d'Ulm, 75248, Paris Cedex 05, France; †Université Paris Descartes/Centre National de la Recherche Scientifique, Faculté de Pharmacie, Laboratoire de Cristallographie et RMN Biologiques (Unite Mixté de Recherche 8015), 4 Avenue de l'Observatoire, 75270 Paris Cedex 06, France; ‡Department of Molecular Physiology and Biophysics, Health Sciences Research Facility, University of Vermont, Burlington, VT 05405-0068; and §Rosenstiel Basic Medical Sciences Research Center, MS 029, Brandeis University, P.O. Box 549110, Waltham, MA 02454-9110

Contributed by Carolyn Cohen, October 24, 2006 (sent for review September 28, 2006)

A 2.5-Å resolution structure of calcium-free calmodulin (CaM) bound to the first two IQ motifs of the murine myosin V heavy chain reveals an unusual CaM conformation. The C-terminal lobe of each CaM adopts a semi-open conformation that grips the first part of the IQ motif (IQxxxR), whereas the N-terminal lobe adopts a closed conformation that interacts more weakly with the second part of the motif (GxxxR). Variable residues in the IQ motif play a critical role in determining the precise structure of the bound CaM, such that even the consensus residues of different motifs show unique interactions with CaM. This complex serves as a model for the lever arm region of many classes of unconventional myosins, as well as other IQ motif-containing proteins such as neuromodulin and IQGAPs.

calcium regulation | semi-open lobe | EF-hand

Myosins are a large family of molecular motors that move along actin filaments. Myosin II ("conventional myosin") generates contraction in muscle, whereas myosin V, an unconventional myosin, transports cargo as a monomer in nonmuscle cells. All myosins have a globular N-terminal motor domain that contains the actin and ATP-binding sites, followed by an elongated α-helical lever arm (lever) (Fig. 1 *Inset*). The lever is composed of special sequences called IQ motifs (consensus sequence IQxxxRGxxxR, consensus residues underlined), each of which is stabilized by the binding of calmodulin (CaM) or a CaM-like light chain. Despite the prevalence of this motif in myosin, there has previously been no atomic-resolution structure of a CaM–myosin heavy chain complex.

The lever arm of myosin V is unusually long with six IQ motifs; this length allows the motor domains to bind 36 nm apart on actin during processive movement. The lever arm amplifies small structural changes originating at the active site and is believed to coordinate interhead communication by means of a strain-dependent mechanism (reviewed in refs. 1 and 2). CaM is also involved in calcium-regulation of myosin V's activity. In the absence of calcium, all six of the IQ motifs of murine myosin V have bound apo-CaM (3). Under these conditions, myosin V adopts a folded, inactive conformation (4–7). Low calcium concentrations unfold and activate the molecule, whereas higher calcium concentrations inhibit motility and processive movement by dissociating CaM from one or more of the IQ motifs (4, 8, 9). Therefore, it is important to know the structure of CaM bound to the IQ motifs to understand more fully both the mechanical and regulatory properties of myosin V.

NMR studies have shown that both lobes of apo-CaM adopt a globular four helix-bundle conformation in the absence of peptide or calcium ions (10, 11). In this so-called "closed" or "almost closed" (12) conformation, hydrophobic residues are buried to hold the bundle together, thus precluding peptide binding. CaM has four high-affinity calcium binding sites called EF-hands, each composed of two α-helices connected by a calcium binding loop (reviewed in ref. 13). Calcium binding to CaM triggers a major change in the orientation of the helices that results in the so-called "open" conformation for both lobes of CaM (10, 11, 14). Solvent exposure of hydrophobic residues in these open lobes forms an effective binding site for the typical CaM-binding target domain, which is a positively charged amphipathic α-helix, with polar and nonpolar surfaces (15).

How then can apo-CaM bind to the IQ motifs of myosin? As anticipated from modeling studies (12, 16, 17), both lobes cannot remain in a closed conformation because CaM needs to grip its target. Here we show that the C-terminal lobe of apo-CaM bound to an IQ motif of the myosin V lever arm adopts a gripping "semi-open" conformation in which a shallow groove allows the IQ motif to fit. The N-terminal lobe is closed. This structure of CaM has not been observed before, and it differs from that of apo-CaM in solution without a peptide. Comparison of the two adjacent IQ/CaM complexes emphasizes the role of nonconserved residues of the IQ motif in target recognition. This structure of the myosin V lever arm serves as a model not only for the large family of proteins that contain IQ motifs including unconventional myosins, neuromodulin, and IQGAPs, but also for the many other sequences that can bind members of the CaM superfamily in the absence of calcium.

Results

Overview of the Structure. The crystal structure of an expressed complex composed of calcium free-CaM bound to the first two IQ motifs of the murine myosin V heavy chain was solved to 2.5-Å resolution. The sequence of the IQ motifs corresponds to the two motifs adjacent to the motor domain of murine myosin V (amino acids Arg-765 to Thr-820) (Fig. 1). Both IQ motifs conform to the consensus sequence (15), which is IQxxxRGxxxR (consensus sequence residues underlined), described as a binding sequence for CaM independent of calcium.

The IQ motifs form a relatively straight α-helix with no sharp bend. The overall topology of the complex is such that the orientation of the IQ motifs and the CaM are antiparallel, with

Author contributions: K.M.T. and C.C. designed research; A.H., E.K., and S.M. performed research; K.M.T. contributed new reagents/analytic tools; A.H., J.-F.G., and S.M. analyzed data; and A.H., K.M.T., and C.C. wrote the paper.

The authors declare no conflict of interest.

Freely available online through the PNAS open access option.

Abbreviation: CaM, calmodulin.

Data deposition: The atomic coordinates have been deposited in the Protein Data Bank, www.pdb.org (PDB ID code 2IX7).

¶Deceased, September 12, 2001.

‖To whom correspondence may be addressed. E-mail: kathleen.trybus@uvm.edu or ccohen@brandeis.edu.

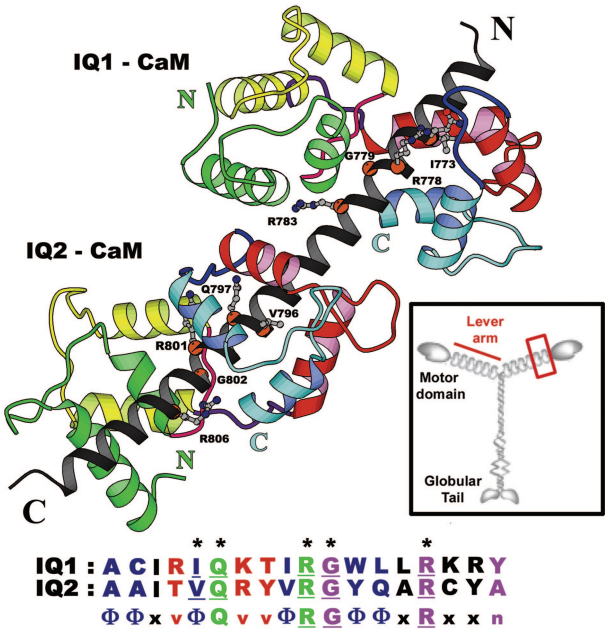

Fig. 1. Structure of the myosin V 2IQ complex. Two CaMs bound in tandem to the two IQ motifs (gray helix) derived from the sequence adjacent to the motor domain of murine myosin V are shown. Consensus sequence residues (*) of the IQ motif are shown in ball and stick. The helices of CaM, designated A–H, are colored in pairs (AB in green, CD in yellow, EF in red, GH in cyan). The orientation of the IQ motifs and CaM are antiparallel. The interlobe linker 2 (purple) joins the N- and C-terminal lobes. Linker 1 (pink, between the B and C helices) and linker 3 (blue, between the F and G helices) interact with consensus residues of the IQ motif. (*Inset*) A cartoon of the myosin V molecule and the region that was crystallized (red box).

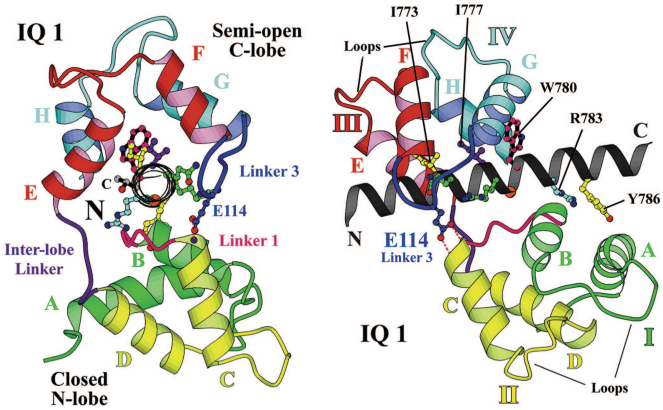

Fig. 2. Conserved features of the CaM / IQ motif recognition. CaM bound to each IQ motif adopts a semi-open C-lobe, and a closed N-lobe. The ribbon diagrams represent CaM (color-coded as in Fig. 1) bound to the first IQ motif in two orthogonal views about the *y* axis. Major interactions with the semi-open C-terminal lobe are: consensus residues Gln-774 and Arg-778 (green) form five hydrogen bonds with main chain atoms in linker 3 (blue), whereas apolar side chains (Ile-773, yellow; Ile-777, purple; Trp-780, black and pink) interact within the hydrophobic C-lobe. Consensus residues Gly-779 (orange ball) and Arg-783 (cyan), as well as Tyr-786 (yellow) interact with the surface of the N-lobe composed of linker 1 (pink) and helix A. Hydrogen bonds between Glu-114 in linker 3 of the C-lobe, and the main-chain nitrogen of Glu-45 and Ala-46 in the N-lobe, provide a sensing mechanism between the two halves of CaM.

the C-terminal lobe (C-lobe, helices E–H) of CaM bound to the more N-terminal region of the IQ motifs (Fig. 1). Each CaM molecule shows unique interactions with its motif, although they both adopt a similar overall conformation. Excluding loop 2, the rmsd between the two N-lobes is 0.5 Å; excluding loop 4, it is 1.2 Å for the C-lobes. The two CaMs are rotated relative to each other by ≈90° relative to the heavy chain helix axis, and interactions between adjacent CaMs are limited to apolar interactions between the A helix of CaM-1 and the F helix of CaM-2. The buried surface area between the two CaMs is 488.4 Å^2. The four calcium-binding loops between pairs of helices of CaM are far from the IQ sequence and do not interact with it. Calcium is not bound to any of the divalent cation binding sites.

An Unusual Conformation of CaM Allows Gripping of the IQ Motif. This structure reveals how calcium-free CaM binds to its target. Compared with the closed conformation described for unbound apo-CaM, the orientation of the F and G helices in the C-lobe changes to form an open groove within the four helix bundle into which the IQ peptide fits (Fig. 2). This semi-open C-lobe interacts tightly with the first part of the IQ motif. The buried surface area of the interaction between the heavy chain and the C-lobe of CaM is 1,918 Å^2 for CaM/IQ1 and 1,913 Å^2 for CaM/IQ2. On the opposite side of the heavy chain helix, the closed N-lobe interacts more weakly with the second part of the IQ-motif target peptide. The buried surface area for the N-lobe is approximately half of that found for the C-lobe: 1,022 Å^2 for CaM/IQ1, and 1,104 Å^2 for CaM/IQ2. Two sites of interaction allow a firm gripping of the peptide by the semi-open C-terminal lobe [Fig. 2 and Supporting Information (SI) Fig. 6]. The hydrophobic cleft within this lobe interacts, for the most part, with apolar residues of the motif, whereas linker 3 (between the F and G helices) of CaM is engaged in numerous van der Waals interactions and five hydrogen bonds with the conserved Gln and Arg residues (IQxxxR) of the motif. Although the residues of the IQ motif found in the C-lobe pocket can vary greatly in sequence, they define a hydrophobic side on the IQ helix as follows, where Φ is an apolar residue: ΦΦxxΦQxxΦRGΦΦ.

A major difference between a semi-open and an open lobe is the depth of the pocket within the lobe surrounding residues Phe-92, Leu-105, Met-124, Ala-128, Phe-141, and Met-144. The signature of the open lobe recognition is the insertion of a large hydrophobic side-chain from the target helix into this deep cleft. In a semi-open lobe, the residues of the IQ motif found near this pocket are not as buried. Nonetheless, residues with a large hydrophobic side chain (Phe, Tyr, Trp, or Met) are generally found at the following two Φ positions of the IQ motif: IQxxΦRGΦ.

By contrast, the N-lobe of CaM retains the closed, nongripping conformation observed for both lobes of apo-CaM in solution studies (10, 11). Additional constraints help maintain the position of the N-lobe close to the peptide. On one side of the IQ helix, the interlobe linker (linker 2) interacts with the heavy chain peptide. On the opposite side, hydrogen bonds between the two lobes of CaM are formed between Glu-114 in linker 3 of the C-lobe and helix C of the N-lobe (Fig. 2). The central region of the IQ motif is thus totally surrounded by CaM.

Variability in N-Lobe Interactions in the Two Consecutive IQ Motifs. Variable residues of the IQ motif (designated "**v**" in **v**IQ**v**-**v**xRGxxxR) play an important role in determining the conformation of the interlobe linker, which in turn alters the position of the N-lobe of CaM (Fig. 3). (Note that residues designated as "x" and "**v**" can be any amino acid, but "**v**" residues influence how the IQ motif is recognized, and "x" residues do not). Consequently, the orientation of the N-lobe of CaM bound to IQ1 differs by ≈20° (relative to the heavy chain helix axis) compared with that seen in IQ2 (Fig. 3). The N-lobe is closer to the IQ peptide in the first motif than in the second, and the number of van der Waals contacts with IQ1 is greater than with

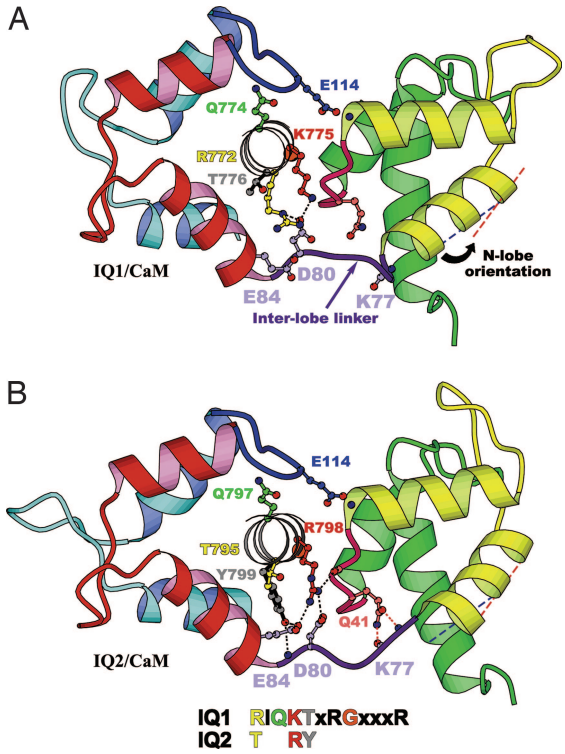

Fig. 3. Variable residues in the IQ motif affect interactions with the interlobe linker and influence the N-lobe orientation of CaM. Ribbon diagrams of CaM bound to the first (*A*) and the second (*B*) IQ motifs display the major differences between the two complexes: a 20° difference in the orientation of the N lobe (relative to the heavy chain helix), and variability in the conformation of the interlobe linker. The last turn of helix D of CaM bound to the second IQ motif is also unfolded. Differences in the sequence of the IQ motif residues (Arg-772/Thr-795, Lys-775/Arg-798, Thr-776/Tyr-799) that interact with the interlobe linker (Asp-80, Glu-84) of CaM cause the N lobe to be further away from the IQ helix in IQ2 compared with IQ1. A key difference for the linker conformation is the substitution of Thr-776 in IQ1 for the bulkier Tyr-799 in IQ2 that interacts specifically with the end of the interlobe linker. The side-chain of Arg-772 in motif 1 forms a hydrogen bond with the sidechain of Asp-80 in the interlobe linker, whereas the smaller Thr-795 in motif 2 cannot do this. The variable Lys-775 in motif 1 forms a hydrogen-bond only with Asp-80, whereas the comparable Arg-798 in IQ2 forms hydrogen-bond with Asp-80 in the interlobe linker as well as Glu-84 in helix E.

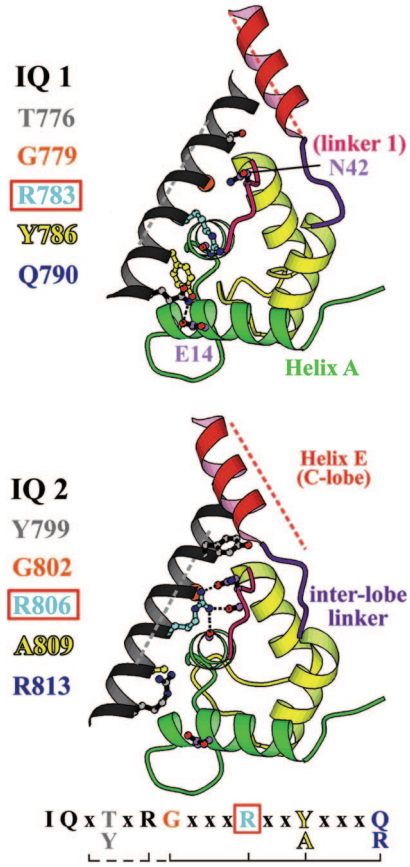

Fig. 4. Binding of the N-lobe of CaM to the second half of the two IQ motifs. The residues involved in N-lobe binding correspond to the second half of the IQ motif, i.e., GWLDRKRYLCMQ for motif 1 (residues 779–790) and GYQARCYAKFLR for motif 2 (residues 802–813). The N-lobes are oriented similarly to compare the interactions made with the IQ motif helix. The variable residues affect the interlobe linker conformation (see Fig. 3), and thus the relative position of the C and N lobes differ in the two complexes. The different orientations are illustrated by a red-dashed line that represents the axis of the E helix of the C lobe as found in IQ1. The gray-dashed line, which represents the axis of the IQ helix as found in IQ2, shows that the IQ helix is further away from the N lobe in motif 2 than in motif 1. Tyr-786 in motif 1 provides additional interactions with helix A that are not found in the second IQ motif, where Tyr is replaced by the smaller Ala. Gln-790 forms a hydrogen bond with Glu-14 on helix A, whereas this interaction does not occur in motif 2 because the side chain of Arg-813 is oriented such that it is ≈7 Å from Glu-14. Even the conserved consensus residue Arg-783 in motif 1 and Arg-806 in motif 2 differ in how they interact with the IQ motif peptide.

IQ2 (Fig. 4 and SI Fig. 6). In both cases, the interface between the N-lobe and the second half of the IQ motif involves residues of linker 1 and helix A in CaM (Fig. 4).

N-lobe interactions differ between IQ motifs because of sequence differences in the variable residues that interact with the N-lobe (designated "**n**" in **n**xxRGxxxRxx**n**xxx**n**) and because of changes in the orientation of the last consensus Arg residue. As noted above, the exact position of the peptide also varies. The last two variable residues (**n**) of the first IQ motif (Tyr-786 and Gln-790) are involved in hydrophobic interactions with helix A of CaM, whereas the corresponding residues in IQ2 (Ala-809 and Arg-813) are too far from the N-lobe of CaM to interact (Fig. 4). In the first IQ motif, the last consensus Arg (Arg-783) forms a hydrogen bond with Ser-38 in linker 1 of CaM. By contrast, the side chain of the equivalent residue in the second IQ motif (Arg-806) forms hydrogen bonds with Arg-37, Gln-41, and Asn-42 (Fig. 4). The consensus Gly residue is very close to linker 1 in both IQ1 and IQ2. Some IQ motifs have large side chain residues at this position (Met in IQ3 and Arg in IQ6), which will further modify the N-lobe orientation and alter the contacts made by the last consensus Arg of the motif.

The finding that interactions between the N-lobe and the IQ consensus residues are not conserved was unexpected, and indicates that the contacts made by the consensus residues of the IQ motif appear to be quite variable.

Calcium and the Semi-Open C-Lobe of CaM. Calcium cannot bind tightly to the semi-open C-lobe because several of the residues involved in chelation are incorrectly oriented. Most importantly, the last (-Z) residues of the Ca^{2+} binding loops, Glu-104 (F helix) and Glu-140 (H helix) of CaM, cannot participate in Ca^{2+} binding without a conformational change (Fig. 5). The F/G helices must adopt an open conformation to bring these residues closer to the Ca^{2+} binding site. The main chain conformation of loop 3 (between helices E and F) in both CaMs of the myosin V structure is similar, and Ca^{2+} binding would not require much change for the side chain of Asp-93, Asp-95, and Asn-97 and the carbonyl of Tyr-99 to participate in calcium binding. By contrast, the main chain conformation of loop 4 (between helices G and H) would require major rearrangements to allow cation binding.

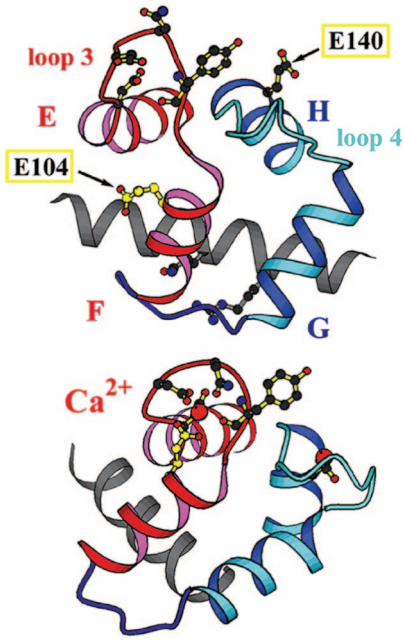

Fig. 5. Conformational change in an EF-hand lobe when Ca^{2+} binds. Comparison of the C-lobe conformation in the semi-open state (*Upper*) and open state (*Lower*; ref. 15), after superimposition of the E helix. Note the difference in the orientation of the four helices (blue) as well as the difference in position of the target peptide (gray). The conformation of loop 3 (between helices E and F) is similar to that found when Ca^{2+} is bound, and most residues involved in Ca^{2+} chelation are in position to participate in binding. The major exception is Glu-104 (yellow) in helix F, which is positioned too far from the rest of loop 3 to coordinate Ca^{2+} in the semi-open lobe. Its recruitment in the coordination sphere requires a major change in the relative orientation of helices E and F. By contrast, the conformation of loop 4 between helices G and H (cyan, *Right*) in the semi-open lobe, greatly differs from that required for Ca^{2+} binding.

Discussion

The 2.5Å resolution crystal structure described here reveals how calcium-free CaM binds to an IQ-motif target peptide. The C-lobe adopts a semi-open conformation that allows gripping of the target peptide in the absence of calcium, and the N-lobe is closed. The presence of the IQ peptide causes the C-lobe to adopt a conformation that differs from that found for unbound apo-CaM (10, 11). Most interactions between the E–H and the F–G helices are lost to allow the opening of a cleft into which the helical IQ motif peptide will fit. The signature of the semi-open lobe conformation is that the IQ motif is gripped by residues at the tip of the lobe near linker 3. The groove is more shallow than in the open state because the helices interact with one another near the calcium-binding loops. By contrast, when CaM is in the calcium-bound "open" state, the target peptide is buried deep within a wide groove of the lobe, and both lobes of CaM play similar roles (15).

The Semi-Open Lobe Conformation and its Specificity of Recognition. The semi-open lobe motif was first described for the calcium-free C-lobes of the myosin essential and regulatory light chains, proteins that are members of the CaM superfamily (17). Earlier modeling studies correctly predicted that this lobe conformation would also be required for apo-CaM to recognize an IQ motif (12). A comparison of CaM and an essential light chain bound to the first IQ motif of myosin V shows very similar semi-open C-lobe conformations (SI Fig. 7). The structure determined here demonstrates that the exact sequence has a large influence on N-lobe position, and thus the precise conformation of CaM and the specific interactions with the IQ motif cannot yet be predicted *a priori*. The apolar residues that interact with the hydrophobic tunnel of the CaM semi-open lobe play the most important role in target recognition, because they define an apolar (Φ) side on the target helix (ΦΦxxΦQxxΦRGΦΦ).

Two other structures show a semi-open EF-hand lobe similar to that described here, but in neither structure can an IQ motif be recognized in the peptide to which CaM is bound. A calcium-free C-lobe of CaM bound to a K^+-channel gating domain adopts a semi-open conformation similar to that in the CaM/IQ motif complex, despite the fact that linker 3 of CaM interacts only with an Arg residue found in place of the consensus Q. The calcium-bound N-lobe has an open conformation that binds to the rest of the target sequence (18). The IQ motifs in some unconventional myosins also differ from the consensus sequence, such as the first IQ motif of myosin X, which has the sequence IRxxxLGxxxR. We infer that CaM binds to such sequences with a semi-open conformation, despite the absence of the consensus sequence residues.

The second structure is an EF hand domain of α-actinin complexed with titin (19). Unlike linker 3 in the CaM/IQ motif complex, the linker between the EF hand domains of α-actinin does not participate in peptide binding. The helices surrounding the linker in α-actinin are one-turn shorter than those of CaM, and thus the linker cannot reach the target. This structure shows that the polar residues that bind to the linker of an EF-hand are not essential features for the gripping of a target helix by a semi-open lobe.

Role of Variable Residues. Two surprising results revealed by this structure are that variable residues of the IQ motif play a critical role in target recognition, and that conserved consensus residues of different IQ motifs can show unique interactions with CaM. Residues variable in sequence ("**v**" in the **v**IQ**v**v**v**xRGxxxR motif) define the conformation of the interlobe linker, which in turn affects how the consensus residues (GxxxR) of the motif interact with the N-lobe. In the current structure, the last consensus R residue of IQ1 and IQ2 interacts very differently with CaM. A structure of the gating domain of a K^+ channel complexed with CaM also demonstrated that substitutions at the Q and R residues (IQxxxR) have no effect on CaM conformation and peptide positioning (18) (see above).

The role that variable IQ residues play in determining CaM affinity for an IQ motif is well illustrated with neuromodulin, which contains an IQ motif that binds apo-CaM. CaM binding is physiologically regulated by PKC phosphorylation on a serine residue of the motif found at the last variable position (IQx**S**xRGxxxR) (20). A negatively charged residue at this position of the IQ motif precludes interactions with the interlobe linker of CaM, which contains negatively charged residues Asp-80 and Glu-84.

Ca^{2+} Binding and EF-Hand Conformation. The C-lobe of unbound apo-CaM binds Ca^{2+} ions with higher affinity than the N-lobe, due to differences in the stability of the closed conformation. When apo-CaM is bound to an IQ motif, it is possible that Ca^{2+} could bind first to the closed N-lobe. The strong interactions between the IQ motif and the C-lobe of CaM would inhibit the transition to an open conformation necessary for Ca^{2+} to bind. Calcium binding to the N-lobe would also disrupt hydrogen bonds between linker 1 and Glu-114 in the C-lobe, thus providing a mechanism by which the C-lobe senses Ca^{2+} binding to the N-lobe of CaM.

Calcium cannot bind tightly to the semi-open lobe conformation without a conformational change, because the conserved Glu residues in the -Z coordination position of the EF hand are not correctly positioned for chelation (Fig. 5). More importantly, we cannot distinguish whether the lobe opens and then calcium

binds, or whether weak calcium binding induces an opening of the lobe.

The Ca^{2+}-induced opening of the C-lobe might allow CaM to remain bound to the lever during this transition, if the hydrophobic residues of the IQ peptide found in the cleft of the semi-open and open lobe remain the same. Most of the Ca^{2+}–CaM/peptide structures would lead one to believe that CaM must dissociate and then rebind to the IQ motif, because calcium binding also changes the order in which the EF-hands of the C-lobe bind to the peptide (SI Fig. 8). Two exceptions are Ca^{2+}–CaM bound to a target peptide from Ca^{2+}–CaM-dependent kinase (21), and Ca^{2+}–CaM bound to the IQ motif of the cardiac Cav1.2 calcium channel (22, 23), both of which show the same polarity for the orientation of the C-lobe as that found in the apo-CaM/IQ motif (SI Fig. 8). Further structural studies are needed to understand more fully how CaM binds to the myosin V IQ motifs in the presence of Ca^{2+}.

IQ Motifs and Calcium-Dependent Regulation of Myosin V. Myosin V forms a folded, inhibited state in the absence of calcium. Whereas low calcium concentrations activate the molecule (4–7), higher calcium levels inhibit motility (4, 24) and terminate processive runs of single myosin V molecules (8, 9). These results are consistent with the idea that calcium significantly weakens the affinity of CaM for one or more of the IQ motifs. Does CaM preferentially dissociate from a particular IQ motif(s) in the presence of calcium? The shortest motor domain–IQ complex that shows calcium sensitivity contains two IQ motifs, implicating site 2 as a site from which CaM dissociates in calcium (25). The buried surface area is similar for both IQ1/CaM and IQ2/CaM (2,878 $Å^2$/2,864 $Å^2$), and thus this apo-structure does not provide a clear explanation for the difference in affinity. It is possible that a more hydrophobic sequence in the second half of the first IQ motif could provide a better anchoring sequence for the N-lobe of Ca^{2+}-CaM. The first IQ motif also has stabilizing interactions with the motor domain in myosin V (26). All of the IQ motifs form a basic amphipathic helix, so that Ca^{2+}–CaM should be able to rebind to any of the IQ motifs, but with different affinities because of sequence variations.

Simply by sequence inspection, it is difficult to predict which other sites (if any) might dissociate their CaM in the presence of calcium. The site showing the most significant deviation from the consensus sequence is IQ6 (IQxxxRGxxxR is replaced by IQxxxR**R**xxx**K**), but this may not affect calcium sensitivity. It has been shown that the presence of a bulky side chain at position 7 and/or the absence of a positively charged residue at position 11 causes the N-lobe of CaM (or a specific light chain) to be in an unusual extended conformation that does not interact with the IQ motif (27). Such unbound N-lobes have been proposed to engage in protein–protein interactions. This extended CaM conformation was not a better fit than the compact form to any of the six CaMs bound to the neck of the inhibited state of murine myosin V (7).

Implications for the Structure of the Myosin V Lever and for Other IQ Containing Proteins. The crystal structure provides a model for the entire myosin V lever, because the overall structure of the 1–2 pair should closely resemble that of the 3–4 and 5–6 pairs of IQ motifs. One feature that does change between IQ motifs, however, is that 23 aa separate IQ motifs 1 and 2, whereas 25 residues separate motifs 2 and 3. This pattern persists along the length of the myosin V lever. When the spacing is 23 aa, as in this structure, the heavy chain helix is straight, and the interactions between adjacent CaMs are limited to residues of the A helix of CaM1 and the F helix of CaM2. A 23-aa spacing is the most common in the myosin superfamily; thus, this structure is likely to be that of the lever for most myosins in the superfamily. Interactions between CaMs bound to motifs 2 and 3 (and 4 and 5) of myosin V, however, will likely differ from what is seen here. When the spacing is longer, the heavy chain may bend so that bare helix is not exposed to the solvent. This feature could give rise to interactions between adjacent CaMs, similar to that seen between the essential light chain and regulatory light chain of myosin II (28). Bending of the lever of myosin V has, in fact, been observed in negatively stained images of myosin V bound to actin, where myosin V adopts a "telemark" aspect (29). By contrast, a "straight-legged" model was favored, based on FIONA analysis of processively walking myosin V (30). This latter observation is consistent with the crystal structure of the second and third IQ motifs from yeast myosin V with bound light chains (MLC1p), which showed a straight helix, and few interactions between light chains, despite a 25-aa spacing (27).

There are a large number of proteins with important cellular roles that bind apo-CaM as well as calcium–CaM. These include unconventional myosins (31), ion channels (32), and IQGAPs (33), where the role of CaM appears to be regulatory. In neuromodulin, the IQ motif may be used for CaM storage and release over a small range of calcium concentration (34, 35). The structure described here is a prototype for CaM interactions with adjacent IQ motifs, and displays yet another of the myriad ways that the ubiquitous protein CaM has evolved to interact with a target peptide.

Materials and Methods

Protein Expression and Purification. The two IQ motifs adjacent to the motor domain of dilute myosin V were cloned into the pGEX-2T (ampicillin resistant, Amersham Pharmacia, Piscataway, NJ) expression vector. The sequence and residue numbers are: A(763)DKLRAACIRIQKTIRGWLLRKRYLCMQRAAITVQRYVRGYQARCYAKFLRRTKAATT(820). The expressed fusion protein consists of GST linked to the two IQ motifs, separated by a thrombin cleavage site. Two amino acids (GS) derived from the vector sequence are added to the N terminus of the IQ motifs after thrombin cleavage. CaM was cloned into a second plasmid that was a derivative of pGP1–2 (kanamycin resistant). Both plasmids were co-transformed into *Escherichia coli* BL21(DE3), and colonies were selected on double-antibiotic (ampicillin and kanamycin) LB agar plates. Cells were grown for 2 h after induction by 0.1 mM IPTG, harvested, and lysed by sonication in cold PBS (10 mM sodium phosphate, pH 7.2/150 mM NaCl) with 1 μM AEBSF and 1 μg/ml leupeptin. The clarified lysate was purified by chromatography on glutathione–Sepharose (Amersham Pharmacia). Thrombin (Roche Molecular Biochemicals, Indianapolis, IN) digestion (10 mg of protein incubated with 20 units of thrombin for 2–3 h at 20°C or overnight at 4°C) was used to remove GST from the IQ motifs. The digestion was stopped with 1 μg/ml leupeptin, and then applied to a glutathione-Sepharose column. The unbound fraction contained the CaM/2IQ complex.

Crystallization and Data Collection. The calcium-free CaM/2IQ complex was crystallized by vapor diffusion at 4°C in a hanging drop format. The drop contained equal volumes of 10 mg/ml protein (10 mM imidazole, pH 7.4/20 mM NaCl/1 mM EGTA/1 mM NaN_3/1 mM DTT/1 μg/ml leupeptin), and the reservoir solution (1.8 M ammonium sulfate/50 mM Mes, pH 5.0/5% MPD/5 mM EGTA/2 mM NaN_3). For data collection at 100 K, crystals were soaked in mother liquor containing 20% glycerol. All data were collected from single cryo-cooled crystals on the A1 beam line at CHESS (see SI Table 1), and autoindexed, scaled, and merged with the programs DENZO and SCALEPACK (36). The crystal structure was solved with the multiple isomorphous replacement method using derivatives prepared by soaking the crystals in heavy atom solutions.

Structure Determination and Refinement. Under similar crystallization conditions, two native nonisomorphous cells were observed with the same space group (forms 1 and 2, which correspond to a small and a large cell). Derivative data were also separated in two sets. Data sets were scaled to native data by Kraut's method (FHSCAL) (35) and analyzed by SCALEIT (37). The heavy atom binding sites were determined from difference isomorphous and anomalous Patterson synthesis using RSPS. In crystal form 1, sites for two isomorphous derivatives Pt and Hg were found and refined with MLPHARE (37). The overall figure of merit was 0.45 in the 15–3.3 Å data range. Density modification (solvent flattening, histogram matching, and skeletonization) was performed with DM (37) and yielded an electron-density map at 4-Å resolution that outlined the right-handed α-helices of the myosin heavy chain and several helices of CaM and confirmed the choice of the "hand" of the derivatives data set. The regulatory domain of scallop myosin (Protein Data Bank ID code 1WCD) was used as an initial model to help build the myosin V neck structure. Density averaging between N-terminal moieties of both CaM improved the map at 4 Å (DM combined figure of merit = 0.52 in 10–3.3 Å data range). The whole structure was built and partially refined by using native structure factors and MIRAS phases as template in CNS (38) (R_{factor}, 40.9%; R_{free}, 44.5%). The structure was then used as a model to solve the second nonisomorphous data set by molecular replacement with AMoRe (39). The structure was refined with CNS to an R-factor of 21.6% (R_{free}, 25.9%) using all independent reflections of the native 2 data set in the 30–2.5 Å data range. At initial stages of the refinement, noncrystallographic symmetry restraints were applied between the CaM subunits, which are related by two NCS operations on their C- and N-terminal moieties. The resolution was gradually extended to the maximum limits of data with grouped temperature factors refinement and a progressive release of NCS constraints. In the latest steps of the refinement, solvent molecules were included in the model and the individual B-factors were also refined. A summary of the refinement statistics is shown in SI Table 2.

This manuscript is dedicated to Suet Mui, who contributed greatly to this work and who died on September 12, 2001, after a long illness. This work was supported by National Institutes of Health Grants AR017346 (to C.C.) and HL38113 (to K.M.T.), a grant from the Muscular Dystrophy Association (to C.C.), and a grant from the French Minister of Research Action Concertee Incitative Biologie Cellulaire, Moléculaire et Structurale (to A.H.). A.H. was also supported by a postdoctoral fellowship from the Human Frontier Sciences Program Organization and the Association Francaise Contre Les Myopathies when at Brandeis University.

1. Trybus KM (2005) *Nat Cell Biol* 7:854–856.
2. Sellers JR, Veigel C (2006) *Curr Opin Cell Biol* 18:68–73.
3. Wang F, Chen L, Arcucci O, Harvey EV, Bowers B, Xu Y, Hammer JA, III, Sellers JR (2000) *J Biol Chem* 275:4329–4335.
4. Krementsov DN, Krementsova EB, Trybus KM (2004) *J Cell Biol* 164:877–886.
5. Wang F, Thirumurugan K, Stafford WF, Hammer JA, III, Knight PJ, Sellers JR (2004) *J Biol Chem* 279:2333–2336.
6. Li XD, Mabuchi K, Ikebe R, Ikebe M (2004) *Biochem Biophys Res Commun* 315:538–545.
7. Liu J, Taylor DW, Krementsova EB, Trybus KM, Taylor KA (2006) *Nature* 442:208–211.
8. Nguyen H, Higuchi H (2005) *Nat Struct Mol Biol* 12:127–132.
9. Lu H, Krementsova EB, Trybus KM (2006) *J Biol Chem* 381:31987–31984.
10. Zhang M, Tanaka T, Ikura M (1995) *Nat Struct Biol* 2:758–767.
11. Kuboniwa H, Tjandra N, Grzesiek S, Ren H, Klee CB, Bax A (1995) *Nat Struct Biol* 2:768–776.
12. Houdusse A, Silver M, Cohen C (1996) *Structure (London)* 4:1475–1490.
13. Grabarek Z (2006) *J Mol Biol* 359:509–525.
14. Finn BE, Evenas J, Drakenberg T, Waltho JP, Thulin E, Forsen S (1995) *Nat Struct Biol* 2:777–783.
15. Meador WE, Means AR, Quiocho FA (1992) *Science* 257:1251–1255.
16. Swindells MB, Ikura M (1996) *Nat Struct Biol* 3:501–504.
17. Houdusse A, Cohen C (1995) *Proc Natl Acad Sci USA* 92:10644–10647.
18. Schumacher MA, Rivard AF, Bachinger HP, Adelman JP (2001) *Nature* 410:1120–1124.
19. Atkinson RA, Joseph C, Kelly G, Muskett FW, Frenkiel TA, Nietlispach D, Pastore A (2001) *Nat Struct Biol* 8:853–857.
20. Chapman ER, Au D, Alexander KA, Nicolson TA, Storm DR (1991) *J Biol Chem* 266:207–213.
21. Osawa M, Tokumitsu H, Swindells MB, Kurihara H, Orita M, Shibanuma T, Furuya T, Ikura M (1999) *Nat Struct Biol* 6:819–824.
22. Van Petegem F, Chatelain FC, Minor DL, Jr (2005) *Nat Struct Mol Biol* 12:1108–1115.
23. Fallon JL, Halling DB, Hamilton SL, Quiocho FA (2005) *Structure (London)* 13:1881–1886.
24. Cheney RE, O'Shea MK, Heuser JE, Coelho MV, Wolenski JS, Espreafico EM, Forscher P, Larson RE, Mooseker MS (1993) *Cell* 75:13–23.
25. Trybus KM, Krementsova E, Freyzon Y (1999) *J Biol Chem* 274:27448–27456.
26. Coureux PD, Wells AL, Menetrey J, Yengo CM, Morris CA, Sweeney HL, Houdusse A (2003) *Nature* 425:419–423.
27. Terrak M, Rebowski G, Lu RC, Grabarek Z, Dominguez R (2005) *Proc Natl Acad Sci USA* 102:12718–12723.
28. Houdusse A, Cohen C (1996) *Structure (London)* 4:21–32.
29. Walker ML, Burgess SA, Sellers JR, Wang F, Hammer JA, III, Trinick J, Knight PJ (2000) *Nature* 405:804–807.
30. Syed S, Snyder GE, Franzini-Armstrong C, Selvin PR, Goldman YE (2006) *EMBO J* 25:1795–1803.
31. Bahler M, Rhoads A (2002) *FEBS Lett* 513:107–113.
32. Soldatov NM (2003) *Trends Pharmacol Sci* 24:167–171.
33. Brown MD, Sacks DB (2006) *Trends Cell Biol* 16:242–249.
34. Estep RP, Alexander KA, Storm DR (1990) *Curr Top Cell Regul* 31:161–180.
35. Black DJ, Leonard J, Persechini A (2006) *Biochemistry* 45:6987–6995.
36. Otwinowski Z (1993) *Data Collection and Processing* (SERC Daresbury Laboratory, Warrington, UK).
37. Collaborative Computational Project 4 (1994) *Acta Crystallogr D* 50:760–763.
38. Brunger AT, Adams PD, Clore GM, DeLano WL, Gros P, Grosse-Kunstleve RW, Jiang JS, Kuszewski J, Nilges M, Pannu NS, *et al.* (1998) *Acta Crystallogr D* 54:905–921.
39. Navaza J (1994) *Acta Crystallogr A* 50:157–163.